

Observation of ψ' decays to $\rho(770)\pi$ and $\rho(2150)\pi$

M. Ablikim¹, J. Z. Bai¹, Y. Ban¹⁰, J. G. Bian¹, X. Cai¹, J. F. Chang¹, H. F. Chen¹⁶, H. S. Chen¹, H. X. Chen¹, J. C. Chen¹, Jin Chen¹, Jun Chen⁶, M. L. Chen¹, Y. B. Chen¹, S. P. Chi², Y. P. Chu¹, X. Z. Cui¹, H. L. Dai¹, Y. S. Dai¹⁸, Z. Y. Deng¹, L. Y. Dong¹, S. X. Du¹, Z. Z. Du¹, J. Fang¹, S. S. Fang², C. D. Fu¹, H. Y. Fu¹, C. S. Gao¹, Y. N. Gao¹⁴, M. Y. Gong¹, W. X. Gong¹, S. D. Gu¹, Y. N. Guo¹, Y. Q. Guo¹, Z. J. Guo¹⁵, F. A. Harris¹⁵, K. L. He¹, M. He¹¹, X. He¹, Y. K. Heng¹, H. M. Hu¹, T. Hu¹, G. S. Huang^{1†}, L. Huang⁶, X. P. Huang¹, X. B. Ji¹, Q. Y. Jia¹⁰, C. H. Jiang¹, X. S. Jiang¹, D. P. Jin¹, S. Jin¹, Y. Jin¹, Y. F. Lai¹, F. Li¹, G. Li¹, H. B. Li^{1‡}, H. H. Li¹, J. Li¹, J. C. Li¹, Q. J. Li¹, R. B. Li¹, R. Y. Li¹, S. M. Li¹, W. G. Li¹, X. L. Li⁷, X. Q. Li⁹, X. S. Li¹⁴, Y. F. Liang¹³, H. B. Liao⁵, C. X. Liu¹, F. Liu⁵, Fang Liu¹⁶, H. M. Liu¹, J. B. Liu¹, J. P. Liu¹⁷, R. G. Liu¹, Z. A. Liu¹, Z. X. Liu¹, F. Lu¹, G. R. Lu⁴, J. G. Lu¹, C. L. Luo⁸, X. L. Luo¹, F. C. Ma⁷, J. M. Ma¹, L. L. Ma¹¹, Q. M. Ma¹, X. Y. Ma¹, Z. P. Mao¹, X. H. Mo¹, J. Nie¹, Z. D. Nie¹, S. L. Olsen¹⁵, H. P. Peng¹⁶, N. D. Qi¹, C. D. Qian¹², H. Qin⁸, J. F. Qiu¹, Z. Y. Ren¹, G. Rong¹, L. Y. Shan¹, L. Shang¹, D. L. Shen¹, X. Y. Shen¹, H. Y. Sheng¹, F. Shi¹, X. Shi¹⁰, H. S. Sun¹, S. S. Sun¹⁶, Y. Z. Sun¹, Z. J. Sun¹, X. Tang¹, N. Tao¹⁶, Y. R. Tian¹⁴, G. L. Tong¹, G. S. Varner¹⁵, D. Y. Wang¹, J. Z. Wang¹, K. Wang¹⁶, L. Wang¹, L. S. Wang¹, M. Wang¹, P. Wang¹, P. L. Wang¹, S. Z. Wang¹, W. F. Wang¹, Y. F. Wang¹, Zhe Wang¹, Z. Wang¹, Zheng Wang¹, Z. Y. Wang¹, C. L. Wei¹, D. H. Wei³, N. Wu¹, Y. M. Wu¹, X. M. Xia¹, X. X. Xie¹, B. Xin⁷, G. F. Xu¹, H. Xu¹, Y. Xu¹, S. T. Xue¹, M. L. Yan¹⁶, F. Yang⁹, H. X. Yang¹, J. Yang¹⁶, S. D. Yang¹, Y. X. Yang³, M. Ye¹, M. H. Ye², Y. X. Ye¹⁶, L. H. Yi⁶, Z. Y. Yi¹, C. S. Yu¹, G. W. Yu¹, C. Z. Yuan¹, J. M. Yuan¹, Y. Yuan¹, Q. Yue¹, S. L. Zang¹, Yu Zeng¹, Y. Zeng⁶, B. X. Zhang¹, B. Y. Zhang¹, C. C. Zhang¹, D. H. Zhang¹, H. Y. Zhang¹, J. Zhang¹, J. Y. Zhang¹, J. W. Zhang¹, L. S. Zhang¹, Q. J. Zhang¹, S. Q. Zhang¹, X. M. Zhang¹, X. Y. Zhang¹¹, Y. J. Zhang¹⁰, Y. Y. Zhang¹, Yiyun Zhang¹³, Z. P. Zhang¹⁶, Z. Q. Zhang⁴, D. X. Zhao¹, J. B. Zhao¹, J. W. Zhao¹, M. G. Zhao⁹, P. P. Zhao¹, W. R. Zhao¹, X. J. Zhao¹, Y. B. Zhao¹, Z. G. Zhao^{1*}, H. Q. Zheng¹⁰, J. P. Zheng¹, L. S. Zheng¹, Z. P. Zheng¹, X. C. Zhong¹, B. Q. Zhou¹, G. M. Zhou¹, L. Zhou¹, N. F. Zhou¹, K. J. Zhu¹, Q. M. Zhu¹, Y. C. Zhu¹, Y. S. Zhu¹, Yingchun Zhu¹, Z. A. Zhu¹, B. A. Zhuang¹, B. S. Zou¹.

(BES Collaboration)

¹ Institute of High Energy Physics, Beijing 100039, People's Republic of China

² China Center for Advanced Science and Technology (CCAST), Beijing 100080, People's Republic of China

³ Guangxi Normal University, Guilin 541004, People's Republic of China

⁴ Henan Normal University, Xinxiang 453002, People's Republic of China

⁵ Huazhong Normal University, Wuhan 430079, People's Republic of China

⁶ Hunan University, Changsha 410082, People's Republic of China

⁷ Liaoning University, Shenyang 110036, People's Republic of China

⁸ Nanjing Normal University, Nanjing 210097, People's Republic of China

⁹ Nankai University, Tianjin 300071, People's Republic of China

¹⁰ Peking University, Beijing 100871, People's Republic of China

¹¹ Shandong University, Jinan 250100, People's Republic of China

¹² Shanghai Jiaotong University, Shanghai 200030, People's Republic of China

¹³ Sichuan University, Chengdu 610064, People's Republic of China

¹⁴ Tsinghua University, Beijing 100084, People's Republic of China

¹⁵ University of Hawaii, Honolulu, Hawaii 96822, USA

¹⁶ University of Science and Technology of China, Hefei 230026, People's Republic of China

¹⁷ Wuhan University, Wuhan 430072, People's Republic of China

¹⁸ Zhejiang University, Hangzhou 310028, People's Republic of China

* Current address: University of Michigan, Ann Arbor, MI 48109, USA

† Current address: Purdue University, West Lafayette, Indiana 47907, USA

‡ Current address: University of Wisconsin at Madison, Madison WI 53706, USA.

(Dated: November 11, 2018)

$\psi' \rightarrow \rho(770)\pi$ is observed for the first time in a data sample of 14 million ψ' decays collected by the BESII detector at the BEPC. The branching fraction is measured to be $\mathcal{B}(\psi' \rightarrow \rho(770)\pi) = (5.1 \pm 0.7 \pm 0.8) \times 10^{-5}$, where the first error is statistical and the second one is systematic. A high mass excited ρ state with mass around 2.15 GeV/ c^2 is also observed with $\mathcal{B}(\psi' \rightarrow \rho(2150)\pi \rightarrow \pi^+\pi^-\pi^0) = (19.4 \pm 2.5^{+11.2}_{-2.1}) \times 10^{-5}$. The branching fraction of $\psi' \rightarrow \pi^+\pi^-\pi^0$ is measured with improved precision, $\mathcal{B}(\psi' \rightarrow \pi^+\pi^-\pi^0) = (18.1 \pm 1.8 \pm 1.9) \times 10^{-5}$. The results may shed light on the understanding of the longstanding “ $\rho\pi$ puzzle” between J/ψ and ψ' hadronic decays.

PACS numbers: 13.25.Gv, 12.38.Qk, 14.40.Gx

From perturbative QCD (pQCD), it is expected that both J/ψ and ψ' decaying into light hadrons are dominated by the annihilation of $c\bar{c}$ into three gluons or one virtual photon, with a width proportional to the square of the wave function at the origin [1]. This yields the pQCD “12% rule”, that is

$$Q_h = \frac{\mathcal{B}_{\psi' \rightarrow h}}{\mathcal{B}_{J/\psi \rightarrow h}} = \frac{\mathcal{B}_{\psi' \rightarrow e^+e^-}}{\mathcal{B}_{J/\psi \rightarrow e^+e^-}} \approx 12\%.$$

A large violation of this rule was first observed in decays to $\rho\pi$ and $K^{*+}K^- + c.c.$ by Mark II [2], *the so called $\rho\pi$ puzzle*. Since then BES has measured many two-body decay modes of the ψ' ; some decays obey the rule while others violate it [3]. There have been many theoretical efforts trying to solve the puzzle [4]. However, none has been accepted as the solution to the problem.

In the study of the $\rho\pi$ puzzle, $\psi' \rightarrow \rho\pi$ is one of the key decay modes and is of great interest to both theorists and experimentalists. A recent calculation of the $\psi' \rightarrow \rho\pi$ branching fraction, done in the framework of SU(3) symmetry, takes into consideration interference between ψ' resonance decays and the continuum amplitude [5]; a branching fraction of $\psi' \rightarrow \rho\pi$ around 1×10^{-4} is predicted with a large error due to the limited precision for ψ' decays into other vector pseudoscalar (VP) modes. The measurement of the $\psi' \rightarrow \rho\pi$ mode is a direct test of many models proposed to solve the $\rho\pi$ puzzle [4, 5].

The data used for this analysis are taken with the Beijing Spectrometer (BESII) detector at the Beijing Electron Positron Collider (BEPC) storage ring operating at the ψ' energy. The number of ψ' events is 14 ± 0.6 million [6], determined from the number of inclusive hadrons, and the luminosity is $(19.72 \pm 0.86) \text{ pb}^{-1}$ as measured by large angle Bhabha events.

BESII is a conventional solenoidal magnet detector that is described in detail in Refs. [7, 8]. A 12-layer vertex chamber (VC) surrounding the beam pipe provides trigger information. A forty-layer main drift chamber (MDC), located radially outside the VC, provides trajectory and energy loss (dE/dx) information for charged tracks over 85% of the total solid angle. The momentum resolution is $\sigma_p/p = 0.017\sqrt{1+p^2}$ (p in GeV/ c), and the dE/dx resolution for hadron tracks is $\sim 8\%$. An array of 48 scintillation counters surrounding the MDC measures the time-of-flight (TOF) of charged tracks with a resolution of ~ 200 ps for hadrons. Radially outside the TOF system is a 12 radiation length, lead-gas barrel shower counter (BSC). This measures the energies of electrons and photons over $\sim 80\%$ of the total solid angle with an energy resolution of $\sigma_E/E = 22\%/\sqrt{E}$ (E in GeV). Outside of the solenoidal coil, which provides a 0.4 Tesla magnetic field over the tracking volume, is an iron flux return that is instrumented with three double layers of counters that identify muons of momentum greater than 0.5 GeV/ c .

A phase space Monte Carlo sample of 2 million $\psi' \rightarrow \pi^+\pi^-\pi^0$ events is generated for the efficiency determination in the partial wave analysis (PWA). Monte Carlo samples of Bhabha, dimuon, and inclusive hadronic events generated with Lundcharm [9] are used for background studies. The simulation of the detector uses a Geant3 [10] based program, which simulates the detector response, including the interactions of secondary particles with the detector material. Reasonable agreement between data and Monte Carlo simulation has been observed in various channels tested, including $e^+e^- \rightarrow (\gamma)e^+e^-$, $e^+e^- \rightarrow (\gamma)\mu^+\mu^-$, $J/\psi \rightarrow p\bar{p}$, and $\psi' \rightarrow J/\psi\pi^+\pi^-$, $J/\psi \rightarrow \ell^+\ell^-$ ($\ell = e, \mu$).

The final state of interest includes two charged pions and one neutral pion which is reconstructed from two photons. The candidate events must satisfy the following selection criteria:

1. A neutral cluster is considered to be a photon candidate when the deposited energy in the BSC is greater than 80 MeV, the angle between the nearest charged track and the cluster is greater than 16° , the first hit of the cluster is in the beginning six radiation lengths of the BSC, and the angle between the cluster development direction in the BSC and the photon emission direction is less than 37° . The angle between two nearest photons is required to be larger than 7° . The number of photon candidates after selection is required to be two.
2. There are two charged tracks in the MDC with net charge zero. A track should have a good helix fit and satisfy $|\cos\theta| < 0.80$, where θ is the polar angle of the track in the MDC.
3. For each charged track, the TOF and dE/dx measurements are used to calculate χ^2 values and the corresponding confidence levels for the hypotheses that the particle is a pion, kaon, or proton ($Prob_\pi$, $Prob_K$, $Prob_p$). At least one charged track is required to satisfy $Prob_\pi > Prob_K$ and $Prob_\pi > Prob_p$. Radiative Bhabha background is removed by requiring the tracks have small dE/dx or small energy deposited in the BSC. Dimuon background is removed using the hit information in the muon counter.
4. A four-constraint kinematic fit is performed under the hypothesis $\psi' \rightarrow \gamma\gamma\pi^+\pi^-$, and the confidence level of the fit is required to be greater than 1%. A Four-constraint kinematic fit is also performed under the hypothesis of $\psi' \rightarrow \gamma\gamma K^+K^-$, and $\chi_{\gamma\gamma\pi\pi}^2 < \chi_{\gamma\gamma KK}^2$ is required to remove $K^+K^-\pi^0$ events.
5. To remove background produced by ψ' cascade decays to J/ψ with $J/\psi \rightarrow \mu^+\mu^-$, the invariant mass of $\pi^+\pi^-$ is required to be less than $2.95 \text{ GeV}/c^2$.

After applying the above selection criteria, the invariant mass distribution of the two photons is shown in Figure 1a. A clear π^0 signal can be seen. A fit to the mass spectrum (shown in Figure 1a) using a π^0 signal shape determined from Monte Carlo simulation and a polynomial background yields $260 \pm 19 \pi^0$ s.

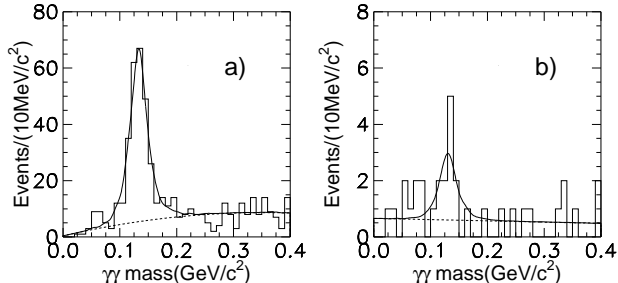


FIG. 1: Two photon invariant mass distribution after final selection for (a) ψ' data and (b) continuum data. The histograms are data, and the curves show the best fits.

The contribution from the continuum [5, 11] is measured using $(6.42 \pm 0.24) \text{ pb}^{-1}$ of data taken at $\sqrt{s} = 3.65 \text{ GeV}$ (continuum data). Figure 1b shows the $\gamma\gamma$ invariant mass distribution and the fit. The number of π^0 from the fit (10.0 ± 4.2) is subtracted incoherently from the ψ' data after normalizing by the two luminosities. This yields 229 ± 23 observed $\psi' \rightarrow \pi^+\pi^-\pi^0$ events.

Dalitz plots of the $\pi^+\pi^-\pi^0$ system for the ψ' and continuum data are shown in Figure 2 after requiring the invariant mass of the two photons lies within $\pm 30 \text{ MeV}/c^2$ of the nominal π^0 mass. (The mass resolution is around $17.5 \text{ MeV}/c^2$ from Monte Carlo simulation.) For the ψ' sample, 250 events are obtained with about 13% non- π^0 background, while for the continuum sample, 11 events are obtained with about 42% non- π^0 background. In ψ' decays, besides clear ρ bands at the edges of the Dalitz plot, there is a cluster of events in the center. This is very different than the Dalitz plot for $J/\psi \rightarrow \pi^+\pi^-\pi^0$ decays [12], indicating different decay dynamics between J/ψ and $\psi' \rightarrow \pi^+\pi^-\pi^0$. There is no clear intermediate state in the continuum data.

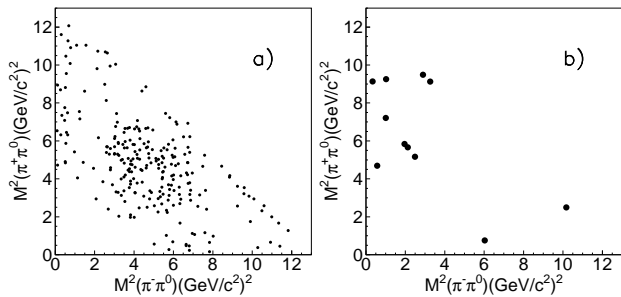


FIG. 2: Dalitz plots of $\pi^+\pi^-\pi^0$ for (a) ψ' data and (b) continuum data after the final selection.

The selected events are fitted in the helicity amplitude formalism with an unbinned maximum likelihood method using MINUIT [13]. For the process

$$\begin{aligned} \psi'(1^-) &\rightarrow \rho(1^-) + \pi(0^-) \\ &\hookrightarrow \pi(0^-) + \pi(0^-), \end{aligned}$$

the intensity distribution dI for the final state is written as

$$dI = \sum_{i=\pm 1} (|A_i|^2 + |C_i|^2) d(LIPS),$$

where C_i is an incoherent background term, that is assumed to be either a constant or to have the same angular distribution as A_i . The difference between these two fits is taken as the systematic error on the background description. $LIPS$ denotes the Lorentz-invariant phase space, and the amplitude

$$A_i = A_i^0(\pi^-, \pi^+) + A_i^+(\pi^+, \pi^0) + A_i^-(\pi^0, \pi^-),$$

where $i = +1$ or -1 is the helicity of the ψ' , the first pion in each set of parentheses is the “designated” pion, and

$$A_{\pm 1}^c = B(m^2) \sin \theta_\pi (\cos \phi_\pi \pm i \cos \theta \sin \phi_\pi) e^{\pm i\phi}.$$

Here $c = 0, +1, \text{ or } -1$ is the net charge of the dipion system, θ and ϕ are the polar and azimuthal angles of the ρ in the ψ' rest frame, θ_π and ϕ_π are the polar and azimuthal angles of the designated pion in the ρ rest frame, and $B(m^2)$ describes the dependence of the amplitude on the dipion mass m :

$$B(m^2) = \frac{BW_{\rho(770)}(m^2) + \sum_j c_j e^{i\beta_j} BW_j(m^2)}{1 + \sum_j c_j},$$

where, $BW(m^2)$ is the Breit-Wigner form of the $\rho(770)$ or its excited states. Here, the Gounaris-Sakurai parameterization [15] is used; β_j and c_j are the relative phase and the relative strength, respectively, between the excited ρ state j and the $\rho(770)$.

Since the number of events is limited, the masses and the widths of all states in the fit are fixed to their PDG values [14], and the number of background events is fixed to the number determined from the $\gamma\gamma$ invariant mass fit. A fit with $\rho(770)$, $\rho(1450)$, $\rho(1700)$ and $\rho(2150)$ results in insignificant $\rho(1450)$ and $\rho(1700)$ contributions. The fit after removing these two components yields a likelihood decrease of 10.7 with four less free parameters. The fit results are shown in Figure 3; the fit describes the data reasonably well.

The fit parameters and results are given in Table I, where for results without errors, the parameter is fixed. The fit yields $(28 \pm 3)\%$ $\rho(770)\pi$ in all $\pi^+\pi^-\pi^0$ events. By comparing the likelihood difference with and without the $\rho(770)\pi$ in the fit, the significance of $\rho(770)\pi$ is determined to be 7.8σ . The significance of $\rho(2150)\pi$ is larger than 10σ .

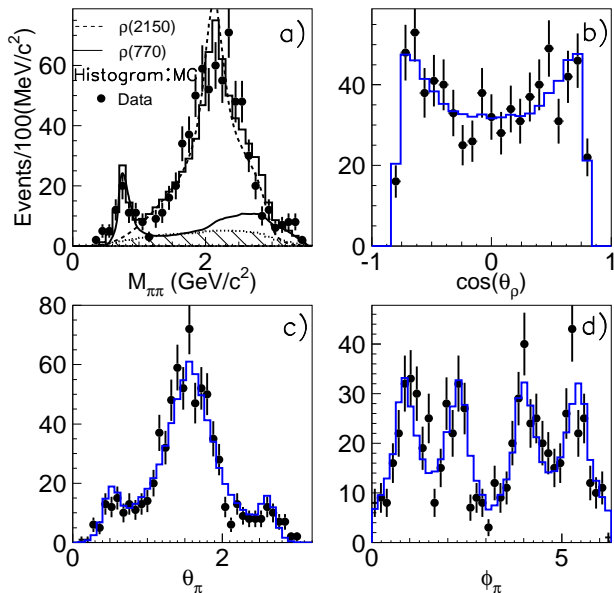


FIG. 3: Comparison between data (dots with error bars) and the final fit (solid histograms) for (a) two pion invariant mass, with a solid line for the $\rho(770)\pi$, a dashed line for the $\rho(2150)\pi$, and a hatched histogram for background; (b) the ρ polar angle in the ψ' rest frame; and (c) and (d) for the polar and azimuthal angles of the designated π in ρ helicity frame.

TABLE I: $\psi' \rightarrow \pi^+\pi^-\pi^0$ fitting parameters and results. For the numbers with no errors, the values are fixed in the fit.

Quantity	Fit result
$M_{\rho(770)}$ (GeV/ c^2)	0.7711
$\Gamma_{\rho(770)}$ (GeV/ c^2)	0.1492
$\beta_{\rho(2150)}$ ($^\circ$)	-102 ± 10
$M_{\rho(2150)}$ (GeV/ c^2)	2.149
$\Gamma_{\rho(2150)}$ (GeV/ c^2)	0.363
$\mathcal{B}(\pi^+\pi^-\pi^0):\mathcal{B}(\rho(770)\pi):\mathcal{B}(\rho(2150)\pi)$	$1:0.28 \pm 0.03:1.07 \pm 0.09$

The fit quality is checked using Pearson's χ^2 test by dividing the Dalitz plots into small areas with at least 20 events and comparing the number of events between data and normalized Monte Carlo simulation. A $\chi^2/\text{ndf} = 14.6/7 = 2.1$ is obtained, which corresponds to a confidence level of 4%. A fit with the $\rho(2150)$ width free; or a fit with $\rho(770)$, $\rho(1450)$, $\rho(1700)$, and $\rho(2150)$; or even with an extra excited ρ state does not improve the fit quality significantly. These cases show that the change in the number of $\rho(770)\pi$ events is less than 9.1%, which is included as part of the systematic error. The number of $\rho(2150)\pi$ events increases by 57% when other excited ρ states are added in the fit due to the interference; this is also included in the systematic error.

Using the parameters of the fit in the Monte Carlo generator, the efficiency of $\psi' \rightarrow \pi^+\pi^-\pi^0$ is estimated to be 9.02%, and the corresponding efficiencies for $\rho(770)\pi$

and $\rho(2150)\pi$ are 10.54% and 8.70%, respectively.

Systematic errors in the $\psi' \rightarrow \pi^+\pi^-\pi^0$ branching fraction measurement come from the kinematic fit, the MDC tracking, charged particle identification, photon identification, background estimation, continuum subtraction, etc. All sources considered are listed in Table II. Most of the errors are measured using clean exclusive J/ψ and ψ' decay samples [12, 16], while some others were described above. For the $\rho(770)\pi$ and $\rho(2150)\pi$, the uncertainties of fitting with different high mass ρ states, etc. are also included. The total systematic error for $\psi' \rightarrow \pi^+\pi^-\pi^0$ is 10.5%, and those for $\psi' \rightarrow \rho(770)\pi$ and $\rho(2150)\pi$ are 16.0% and $^{+58.0}_{-10.6}\%$, respectively.

TABLE II: Summary of systematic errors on $\mathcal{B}(\psi' \rightarrow \pi^+\pi^-\pi^0)$.

Source	Relative error (%)
Trigger	0.5
MDC tracking	4.0
Kinematic fit	6.0
Photon efficiency	4.0
Number of photons	2.0
Background estimation	3.6
Particle ID	negligible
Total number of ψ'	4.0
Continuum subtraction	3.0
Total	10.5

Using the numbers obtained above, the branching fractions of $\psi' \rightarrow \pi^+\pi^-\pi^0$, $\rho(770)\pi$ and $\rho(2150)\pi$ are

$$\begin{aligned} \mathcal{B}(\pi^+\pi^-\pi^0) &= (18.1 \pm 1.8 \pm 1.9) \times 10^{-5}, \\ \mathcal{B}(\rho(770)\pi \rightarrow \pi^+\pi^-\pi^0) &= (5.1 \pm 0.7 \pm 0.8) \times 10^{-5}, \\ \mathcal{B}(\rho(2150)\pi \rightarrow \pi^+\pi^-\pi^0) &= (19.4 \pm 2.5^{+11.2}_{-2.1}) \times 10^{-5}, \end{aligned}$$

where the first errors are statistical and the second systematic.

Our $\mathcal{B}(\psi' \rightarrow \pi^+\pi^-\pi^0)$ agrees with the Mark II [2] result within 1.8σ , and $\mathcal{B}(\psi' \rightarrow \rho(770)\pi)$ is below the Mark II [2] upper limit and in agreement with one model prediction [5]. It should be noted that the continuum amplitude which is considered incoherently in this analysis could increase the $\rho(770)\pi$ branching fraction due to interference with the resonance [5]. This should be considered in a higher statistics experiment.

Comparing with the corresponding J/ψ decay branching fractions, it is found that both $\pi^+\pi^-\pi^0$ and $\rho(770)\pi$ are highly suppressed compared with the ‘‘12% rule’’, while for $\rho(2150)\pi$, there is no measurement in J/ψ decays. It could be enhanced in ψ' decays since the phase space in J/ψ decays is limited due to the large mass of the excited ρ state. It should be noted that using the J/ψ and $\psi' \rightarrow \rho\pi$ branching fractions, the $\psi'' \rightarrow \rho\pi$ branching fraction and the $e^+e^- \rightarrow \rho\pi$ cross section at $\sqrt{s} = 3.773$ GeV can be predicted in the S - and D -wave

mixing model [17], which is proposed as a solution of the $\rho\pi$ puzzle in ψ' decays.

In summary, $\psi' \rightarrow \rho(770)\pi$ is observed in ψ' decays for the first time, and the branching fraction is measured to be $\mathcal{B}(\psi' \rightarrow \rho(770)\pi) = (5.1 \pm 0.7 \pm 0.8) \times 10^{-5}$. A high mass excited ρ state at mass around $2.15 \text{ GeV}/c^2$ is also observed with $\mathcal{B}(\psi' \rightarrow \rho(2150)\pi \rightarrow \pi^+\pi^-\pi^0) = (19.4 \pm 2.5_{-2.1}^{+11.2}) \times 10^{-5}$. The results may shed light on the understanding of the longstanding “ $\rho\pi$ puzzle” between J/ψ and ψ' hadronic decays.

The BES collaboration thanks the staff of BEPC for their hard efforts and the members of IHEP computing center for their helpful assistance. This work is supported in part by the National Natural Science Foundation of China under contracts Nos. 19991480, 10225524, 10225525, the Chinese Academy of Sciences under contract No. KJ 95T-03, the 100 Talents Program of CAS under Contract Nos. U-11, U-24, U-25, and the Knowledge Innovation Project of CAS under Contract Nos. U-602, U-34 (IHEP); by the National Natural Science Foundation of China under Contract No. 10175060 (USTC), and No. 10225522 (Tsinghua University); and by the US Department of Energy under Contract No. DE-FG03-94ER40833 (U Hawaii).

-
- [1] T. Appelquist and H. D. Politzer, Phys. Rev. Lett. **34**, 43 (1975); A. De Rújula and S. L. Glashow, Phys. Rev. Lett. **34**, 46 (1975).
 [2] M. E. B. Franklin *et al.* (Mark II Collab.), Phys. Rev. Lett. **51**, 963 (1983).
 [3] Many results may be found in Ref. [14]; more recent results may be found in J. Z. Bai *et al.*, (BES Collab.),

- Phys. Rev. D **69**, 072001 (2004); J. Z. Bai *et al.*, (BES Collab.), Phys. Rev. Lett. **92**, 052001 (2004); and M. Ablikim *et al.*, (BES Collab.), hep-ex/0407037.
 [4] W. S. Hou and A. Soni, Phys. Rev. Lett. **50**, 569 (1983); S. J. Brodsky and M. Karliner, Phys. Rev. Lett. **78**, 4682 (1997); M. Chaichian and N. A. Törnqvist, Nucl. Phys. B **323**, 75 (1989); S. S. Pinsky, Phys. Lett. B **236**, 479 (1990); G. Karl and W. Roberts, Phys. Lett. B **144**, 243 (1984); X. Q. Li, D. V. Bugg and B. S. Zou, Phys. Rev. D **55**, 1421 (1997); J. M. Gérard and J. Weyers, Phys. Lett. B **462**, 324 (1999); T. Feldmann and P. Kroll, Phys. Rev. D **62**, 074006 (2000).
 [5] P. Wang, C. Z. Yuan and X. H. Mo, Phys. Rev. D **69**, 057502 (2003).
 [6] X. H. Mo *et al.* High Ener. Phys. and Nucl. Phys. **27**, 455 (2004), hep-ex/0407055.
 [7] J. Z. Bai. *et al.* (BES Collab.), Nucl. Instr. Meth. A **344**, 319 (1994).
 [8] J. Z. Bai. *et al.* (BES Collab.), Nucl. Instr. Meth. A **458**, 627 (2001).
 [9] J. C. Chen *et al.*, Phys. Rev. D **62**, 034003 (2000).
 [10] “GEANT: detector description and simulation tool”, V3.21, CERN program library long writeup W5013. Oct. 1994.
 [11] P. Wang, C. Z. Yuan, X. H. Mo and D. H. Zhang, Phys. Lett. B **593**, 89 (2004).
 [12] J. Z. Bai *et al.*, (BES Collab.), Phys. Rev. D **70**, 012005 (2004).
 [13] CERN Program Library Long Writeup D506
 [14] S. Eidelman *et al.* (Particle Data Group), Phys. Lett. B **592**, 1 (2004).
 [15] G. J. Gounaris and J. J. Sakurai, Phys. Rev. Lett. **21**, 244 (1968).
 [16] J. Z. Bai *et al.*, (BES Collab.), Phys. Rev. D **69**, 072001 (2004).
 [17] P. Wang, X. H. Mo and C. Z. Yuan, Phys. Lett. B **574**, 41 (2003).